Bacterial exonuclease □ expands its enzymatic activities on single-stranded DNA

Hao Wang [1], Chen Ye [1], Qi Lu [2], Zhijie Jiang [1], Chao Jiang [3], Chun Zhou [4], Na Li [1], Caiqiao Zhang [1], Guoping Zhao [5, 6, 7], Min Yue [1, 2, 5] *, Yan Li [1, 2,] *

[1] Department of Veterinary Medicine, Zhejiang University College of Animal Sciences, Hangzhou, China

[2] Hainan Institute of Zhejiang University, Sanya, China

[3] Life Sciences Institute, Zhejiang University, Hangzhou, Zhejiang, 310058, China

[4] School of Public Health, and Department of Pathology of Sir Run Run Shaw Hospital, Zhejiang University School of Medicine, Hangzhou, Zhejiang, 310058, China.

[5] School of Life Science, Hangzhou Institute for Advanced Study, University of Chinese Academy of Sciences, Hangzhou, 310024, China;

[6] CAS Key Laboratory of Synthetic Biology, Institute of Plant Physiology and Ecology, Shanghai Institutes for Biological Sciences, Chinese Academy of Sciences, Shanghai 200031, China;

[7] Department of Microbiology and Microbial Engineering, School of Life Sciences, Fudan University, Shanghai 200433, China;

[8] State Key Laboratory for Diagnosis and Treatment of Infectious Diseases, National Clinical Research Center for Infectious Diseases, National Medical Center for Infectious Diseases, The First Affiliated Hospital, College of Medicine, Zhejiang University, Hangzhou, China

* Correspondence

Min Yue (myue@zju.edu.cn), Zhejiang University Department of Veterinary Medicine, 866 Yuhangtang Rd, Hangzhou 310058, P.R. China

Yan Li (yanli3@zju.edu.cn), Zhejiang University Department of Veterinary Medicine, 866 Yuhangtang Rd, Hangzhou 310058, P.R. China

Abstract

Bacterial exonuclease □ (Exo□), widely acknowledged for specifically targeting double-stranded DNA (dsDNA), has been documented as a DNA repair-associated nuclease with apurinic/apyrimidinic (AP)-endonuclease and 3′→5′ exonuclease activities. Due to these enzymatic properties, Exo□ has been broadly applied in molecular biosensors. Here, we demonstrate that Exo□ (*Escherichia coli*) possesses highly active enzymatic activities on ssDNA. By using a range of ssDNA fluorescence-quenching reporters and fluorophore-labelled probes coupled with mass spectrometry analysis, we found Exo□ cleaved the ssDNA at 5′-bond of phosphodiester from 3′ to 5′ end by both exonuclease and endonuclease activities. Additional point mutation analysis identified the critical residues for the ssDNase action of Exo□ and suggested the activity shared the same active center with the dsDNA-targeted activities of Exo□. Notably, Exo□ could also digest the dsDNA structures containing 3′-end ssDNA. Considering most Exo□-assisted molecular biosensors require the involvement of single-stranded DNA (ssDNA) or nucleic acid aptamer containing ssDNA, the activity will lead to low efficiency or false positive outcome. Our study revealed the multi-enzymatic activity and the underlying molecular mechanism of Exo□ on ssDNA, illuminating novel insights for understanding its biological roles in DNA repair and the rational design of Exo□-ssDNA involved diagnostics.

Keywords: Exonuclease □ (Exo□); Fluorescence-quenching reporter; Single-stranded DNA (ssDNA); Exonuclease and endonuclease activity; Exo□-based diagnostics; DNA repair

INTRODUCTION

Endogenous and exogenous stresses frequently result in DNA damage. Base damage is one of the most common DNA lesions caused by alkylation, oxidation, deamination, and depurination/depyrimidination [1]. Such structural changes in double-stranded DNA (dsDNA) immediately recruit a range of downstream enzymes to the lesion locus for repair, a process known as base excision repair (BER) [2]. Exonuclease □ (Exo□) has been widely recognized as one of the most critical players in BER [3-5]. Based on the enzymatic activities involved, BER has been conceptually divided into the following five steps [6]: 1) glycosylase excision on the damaged base forming the apurinic/apyrimidinic (AP) site; 2) AP endonuclease (Exo□) incision on the phosphodiester backbone to create and extend a ssDNA gap; 3) 5′-deoxyribose phosphate (dRp) removal; 4) polymerase-directed gap filling; 5) ligase-aided nick sealing. During the BER process, Exo□ performs the dual roles of AP endonuclease and exonuclease in *E. coli* [7]. Once the damaged bases are removed by glycosylases leaving an AP site, Exo□ first acts as an endonuclease to hydrolyze the phosphodiester bond at the 5′-end of the AP site, then as an exonuclease to degrade the downstream single-stranded DNA (ssDNA) of the duplex region from 3′ to 5′ end. These two Exo□-dominated enzymatic activities create a proper length of ssDNA gap on dsDNA, which is required for polymerase binding at the locus to re-synthesize nucleotides [8]. Structural analysis revealed that the α_M helix of Exo□ stabilized the substrate by stretching into the major groove of dsDNA in the catalytic process [5]. Interestingly, different from the typical multifunctional enzymes, i.e., DNA polymerase [9], with separate active sites, the multiple activities of Exo□ on dsDNA lie in the same active site [4, 5].

During the 1960s-1990s, Kornberg's laboratory demonstrated that Exo□ specifically recognizes dsDNA but is inactive to ssDNA based on an ssDNA oligo of five consecutive Ts (5′ pTpTpTpTpT 3′) [10, 11], and other researchers showed Exo□ had limited enzymatic activity on dsDNA containing 3′-protruding ssDNA (≥ 4 nt) [12, 13]. Hence, Exo□ was previously proposed to produce ssDNA from dsDNA [14]. Combined with novel materials, chemicals, or mechanical platforms, Exo□ has been widely employed in detecting nucleic acids, metals, toxins, and other types of small molecules [15]. Based on the specific enzymatic activities of Exo□ on dsDNA in detections, the Exo□-assisted biosensors can be divided into two categories: AP-endonuclease and exonuclease-based methods. As a promising replacement for PCR technique[16], TwistAmp® Liquid exo kit (https://www.twistdx.co.uk/product/twistamp-liquid-exo/)

represents one of the most successful AP-endonuclease-based nucleic acid detection, which combines recombinase polymerase amplification (RPA) [17] and Exo□. In the application of the commercial kit, a 46~52 nt ssDNA probe is required to base-pair with the target sequence and the probe should also contain an AP site (usually simulated by a tetrahydrofuran [THF] residue) labelled with a fluorophore and a quencher, respectively, at or near the 5′- and 3′- end of AP. Once the ssDNA probe binds to the complementary sequence with the aid of recombinase and forms a dsDNA region containing an AP, Exo□ recognizes and cleaves the AP site, which separates the fluorophore and quencher, leading to a fluorescence release. In the exonuclease-based methods, ssDNA or nucleic acid aptamer contained ssDNA is often configured to form dsDNA substrate for the exonuclease activity of Exo□ [15]. However, the digesting of Exo□ on ssDNA probe has been inadvertently observed in three Exo□-developed detection methods [18-20] and a biochemical study [21]. As the studies displayed limitations in proving the ssDNase activity of Exo□: a) no additional procedure safeguards the ssDNA substrate from forming a secondary structure containing dsDNA duplex in or between ssDNA, which can easily happen, and b) only stays on the phenomenon without further in-depth characterization and mechanism exploring, Exo□ has therefore still been publicly described (https://www.sciencedirect.com/topics/biochemistry-genetics-and-molecular-biology/exonuclease-□), studied [3, 4, 8, 22], and commercialized as a dsDNA-specific enzyme that is inactive or has limited activity on ssDNA (https://www.thermofisher.cn/order/catalog/product/EN0191 and https://international.neb.com/products/m0206-exonuclease-iii-e-coli#Product%20Information) for over a half-century. The definition of the enzymatic activity of Exo□ on ssDNA remains ambiguous.

To address this long-standing controversy, we used several sensitive fluorescence-quenching (FQ) ssDNA reporters to detect the enzymatic activity of Exo□ on ssDNA. FQ is distance-dependent, where increasing the distance between the fluorophore and the quencher increases the fluorescence intensity. As a sensitive and visible physical phenomenon, it has been transformed into one of the most influential techniques for monitoring dynamic alterations of macromolecule conformation in complex interactions [23-25]. The DNA or RNA-constructed FQ reporter has been successfully employed in CRISPR-based diagnostics [26, 27] as an efficient sensor of collateral trans-cleavage activity of Cas12a on ssDNA [28] and Cas13a on RNA [29]. Once the nuclease cuts the ssDNA or RNA connector and disconnects the fluorophore and quencher, fluorescence will be significantly released as a positive readout for the de-

tection. Combining with mass spectrometry and structure analysis, our finding demonstrated the ssDNase activity of Exo□ and its potential biological role in DNA repair. Furthermore, it also alerted a risk of false positive or low efficiency within the widely adopted Exo□-ssDNA combined diagnostic approach.

RESULTS

Exo□ rapidly cleaved the ssDNA FQ reporters

As an ultrasensitive biosensor of the ssDNase activity, the ssDNA FQ **(Figure 1A)** (5 nt) of CRISPR-based detection systems[26] were utilized for assaying the ssDNase activity of Exo□ and its digesting rate. To examine if the substrates form the dsDNA region internally or between ssDNA strands, the dsDNA-specific nuclease T7 exo[30] was used as the negative control, while LbCas12a[28] was designated as the positive control. Once the ssDNA FQ reporter is cleaved by nuclease, the fluorescent signal will be released. In contrast to T7 exo and LbCas12a, Exo□ (5 U/μl) triggered a substantial fluorescent signal promptly upon adding to FQ reporter (5 μM) (a total of 50 pmol), and most of the ssDNA substrate (over 90%) was cleaved in the first minute **(Figure 1B)**, which suggested that the commercial Exo□ (5 U/μl) degraded over 2.7×10^{13} (45 pmol) phosphodiester bonds per minute in the reaction, significantly faster than 0.7 pmol phosphodiester bonds per minute of LbCas12a and that of other nucleases **(Figure 1C)**. Strikingly, we found even at room temperature (22°C), the fluorescence release initiated immediately when 0.5 μl Exo□ was mixed with FQ reporter (5 μM) under LED blue light **(Supplementary video S1)**. In summary, T7 exo showed no significance with D-T7 exo; APE1 exhibited a significantly detectable fluorescence signal compared to its deactivated counterpart (D-APE1), albeit much weaker than that of Exo□ and LbCas12a **(Figure 1C)**.

Given that Exo□ has long been recognized as a dsDNA-specific nuclease, we initially speculated that the ssDNA activity on FQ reporters might be ascribed to its cleavage at the 5′ or 3′ end phosphodiester bonds of ssDNA reporter rather than the typical phosphodiester bonds within ssDNA**.** To narrow down the possibility, we first removed the 5′ end phosphodiester by designing the FQ reporter with FAM labelled at its 5′ first thymine (T_1) base instead of the 5′ end phosphate **(Figure 1D)**. Logically, the 5′ FAM T_1-labelled reporter should not produce fluorescence if Exo□ cuts at the 5′ end phosphodiester bond. But fluorescence monitoring assays showed that Exo□ (5 U/μl) digested over 90% of 5′ FAM T_1-labelled FQ reporter (5 μM) in the first minute **(Figure 1E)**, indicating a speed of 2.7×10^{13} (45 pmol) phosphodiester bonds per mi-

nute **(Figure 1F)**; APE1 and LbCas12a also exhibited a stronger fluorescence intensity compared to their deactivated counterparts (D-APE1 and D-LbCas12a) **(Figure 1F)**. Treated with Exo□, the fluorescence of the FQ reporter was generated rapidly even before incubating at 37°C **(Supplementary video S2)**. The evidence implied that Exo□ cleaved the FQ reporter not at 5′ end phosphodiesters.

Subsequently, we removed the 3′ end phosphodiesters by labelling the BHQ1 at the reporter's 3′ end thymine **(Figure 1G)**. The fluorescence monitoring assay showed that the Exo□-treated FQ reporter (5 μM) released a significant fluorescence signal compared to other nucleases. Slower than the previous two FQ reporters, it cleaved over 90% of the base-labelled FQ reporter in 10 min **(Figure 1H)**, demonstrating that the commercial Exo□ (5 U/μl) digested about 2.7×10^{12} (4.5 pmol) phosphodiester bonds or nucleotides of ssDNA in the FQ reporter **(Figure 1I)**. Compared with the massive fluorescence induced by Exo□, the modifications on thymine may impede the binding and cleaving of the LbCas12a-crRNA complex on the ssDNA substrate, leading to less fluorescence generated **(Figure 1I)**. Combining all the results of three types of FQ reporters, we demonstrated Exo□ might harbor a powerful ssDNase activity.

Exo□ is an efficient 3′→5′ ssDNase

To exclude the possibility of sequence-specific driven catalysis of Exo□, we tested three ssDNA oligos with fluorophore labelled at the 5′ end (5 μM) **(Figure 2A)**. After 40 min of incubation with Exo□ (5 U/μl) at 37°C, the reaction mixture of three probes was separated by gel electrophoresis. The result indicated that the ssDNA was degraded by Exo□ and LbCas12a compared with the undigested product of APE1 and T7 exo **(Figure 2B and 2C)**. The reaction products gradually decreased in length as time prolonged **(Figure 2D)**, suggesting that Exo□ shortened Probe 1 into smaller fragments gradually and rapidly from 3′ to 5′ end. The time course analysis on the digestion demonstrated the digesting rate of Exo□ on the ssDNA stood at 20~400 pmol nucleotides per minute in the 15 min **(Figure 2E)**. Similarly, Probe 2 was processed into shorter fragments by Exo□ and LbCas12a compared to other nucleases **(Figure 2F and 2G)** and were digested gradually and promptly over time **(Figure 2H and 2I)**. Probe 3 also resembled the digestion over time **(Figure 2J, 2K, 2L, and 2M)**. The gradual and successive degradation on the three ssDNA substrates in the 40 min indicated that Exo□ (5 U/μl) digested the ssDNA (5 μM) in the 3′→5′ direction with an estimated average speed of approximately 1.5×10^{13} (25 pmol) phosphodiester bonds

or nucleotides per minute, and the digestion rate varied with the encountered nucleotides of ssDNA subatrate. We also compared the digestion rates of Exo□ on ssDNA and dsDNA. The result showed that Exo□ required 10 minutes to digest the 30-nt single-stranded DNA (ssDNA) (**Supplementary Figure S1A**), whereas it could digest the same sequence on double-stranded DNA (dsDNA) within 1 minute (**Supplementary Figure S1B**). This indicated that Exo□ digested the dsDNA at a rate at least ten times faster than ssDNA. Even not as rapid as the dsDNA, the ssDNase activity of Exo□ surpasses that of the conventional ssDNA-specific nuclease ExoI [20], suggesting a potential biological significance of Exo□ in bacteria related to ssDNA.

To investigate the massive disparity of ssDNase activity between the two highly similar homologs, Exo□ and APE1, we performed structure alignment and found the structure of the α_M helix of Exo□ deteriorated in APE1 **(Figure 2N)**. As α_M lies in the binding interface of Exo□ and substrate [5], it might play a critical role in the digestion of ssDNA. The degenerated ssDNA-cleavage activity of APE1 may evolve to minimize the risk of genomic instability in human. Whether it is associated with related human cancers remains to be further studied.

Mass spectrometry analysis revealed the endonuclease activity of Exo□ on ssDNA

To provide high-resolution information regarding the Exo□ actions on the ssDNA substrates (used in Figure 2), we parsed the products of Exo□ by ESI-mass spectrometry. The major products of the three ssDNA probes are identified and listed (**Supplementary Table S1)** and all the reaction products are included in **Supplementary File S1**. After being treated with Exo□, Probe 1 was digested to the three major products (Product 1 of Probe 1, termed as P1P1, Mass peak = 2914.9 Da; P1P2, Mass peak = 2601.5 Da; P1P3, Mass peak = 5395.5 Da) **(Figure 3A),** which respectively matched to an 8-nt (Theoretical mass = 2915.6 Da), 7-nt (Theoretical mass = 2602.4 Da) and 16-nt (Theoretical mass = 5397.2 Da) ssDNA fragments of Probe 1, and these undigested nucleatides accounted for ~15% of the input **(Figure 3B)**. Probe 2 was digested to two major products (P2P1, Mass peak = 4639.6 Da; P2P2, Mass peak = 957.7 Da) **(Figure 3C)**, which respectively matched to a 13-nt (Theoretical mass = 4641.6 Da) and 3-nt (Theoretical mass = 957.6 Da) ssDNA fragments of Probe 2, and these remaining oligos accounted for ~0.6% of the input **(Figure 3D)**. Probe 3 was digested into four products (P3P1, Mass peak = 2936.9; P3P2, Mass peak = 3240.9; P3P3, Mass peak = 2632.7; P3P4, Mass peak = 2328.7) **(Figure 3E)** respectively matched to an 8-nt (Theoretical mass = 2937.6 Da), 9-nt (Theoretical mass = 3241.8

Da), 7-nt (Theoretical mass = 2633.4 Da) and 6-nt (Theoretical mass = 2329.2 Da) fragments of Probe 3, and these leftover accounted for ~28% of the input **(Figure 3F)**. According to the mass peak intensities of reaction products **(Supplementary Table S2)**, the majority of ssDNA substrates (5 μM) were degraded into mononucleotides (~85% for Probe 1, ~99% for Probe 2 and ~72% for Probe 3) by Exo□ (5 U/μl). As the control, the mass spectrometry analysis of the three probes without Exo□ digestion is provided **(Supplementary Figure S2A, S2B, and S2C)**.

Furthermore, we found these undigested fragments above (P1P1, P1P2, P2P1, P3P1, P3P2, P3P3, and P3P4) retained an intact 5′ end fluorophore and a free 3′-OH, which indicated the Exo□ catalyzed the cleavage of ssDNA at the 5′-side bond of phosphodiester. And 17 ssDNA fragments (4 fragments from Probe 1 and 13 fragments from Probe 2 included in **Supplementary File S1**) were identified from the middle part of the ssDNA, impling Exo□ possessed an endonuclease activity on ssDNA, which might be activated by specific sequences. Combined with the results of Figure 2, we confirmed that Exo□ is an efficient ssDNase, and its digestion rate varied based on the sequences of ssDNA.

Reaction conditions for the ssDNase activity of Exo□

To explore if this enzymatic action of Exo□ requires Mg^{2+}, we added EDTA to the enzymatic reaction. The endpoint fluorescence intensity of the FQ reporter showed that the addition of EDTA completely inhibited the fluorescence generation compared with the reaction without EDTA **(Figure 4A)**. The gel analysis on the cleavage product of three ssDNA probes showed that adding EDTA stopped the catalytic digestion of Exo□ on ssDNA **(Figure 4B)**. These EDTA-added experiments demonstrated that Mg^{2+} was required for the ssDNase activity of Exo□. Subsequently, we added different concentrations of Exo□ (0, 0.025, 0.125, 0.250, 0.500, and 1.250 μM) to the ssDNA probe (0.5 μM). The result showed the amount of Exo□ (0.025 μM) degraded ~10 nucleotides of ssDNA substrate (0.5 μM) in 10 min **(Figure 4C and 4D)**, suggesting each molecular of Exo□ was capable of cleaving off one nucleotide by 3 seconds. To explore the suitable temperature for the ssDNase activity, Exo□ was incubated with the ssDNA probe at 0, 16, 25, 37, 42, and 50°C, respectively. The gel results indicated the ssDNase activity of Exo□ was active at 16, 25, and 37°C but receded when the temperature was raised to 42°C and 50°C **(Figure 4E and 4F)**, suggesting the suitable temperature for the ssDNase activity of Exo□ was probably at a range of 16~42°C.

Intriguingly, focusing on the major products of the three ssDNA probes in Figure 3, we found digestion of Exo□ seemingly always stalled in or ahead of a zone of serial identical bases **(Supplementary Table S1)**, suggesting this type of sequence feature might affect the digestion of Exo□. To explore if this phenomenon always occurs upon serial identical bases, we performed enzymatic reactions on three 5′ FAM-labelled ssDNA probes consisting of 20 nt identical nucleotides. The reaction product was analyzed by gel after these ssDNA substrates (5 μM) were incubated with purified Exo□ (2.5 μM) for 15 min. The result of the time course analysis indicated that A_{20}, C_{20}, and T_{20} displayed an obviously slower degradation than the ssDNA substrates in Figure 2 ($A_{20} \approx C_{20} > T_{20}$) **(Figure 4G and 4H)**, suggesting the consecutive identical nucleotides in ssDNA might slow down the digestion of Exo□.

Exo□ in the commercial isothermal amplification diagnostic kits digested the ssDNA FQ reporter and probes

Due to the well-acknowledged dsDNA activities of Exo□, most Exo□-assisted diagnostic methods require ssDNA to form an appropriate dsDNA intermediate (**Supplementary Table S2**). As a promising replacement for PCR technique [16], RPA [17, 31], and MIRA [32, 33] kits, as well as their derivative products, the MIRA- and RPA-Exo□ kits [34, 35], have been widely used for nucleic acid detection. To explore if Exo□ contained in the commercial detection kits digests the ssDNA probe or primer, we used an FQ reporter and 5′ FAM-labelled ssDNA probes to test the commercial kits of MIRA-Exo□ and RPA-Exo□, while the RPA and MIRA detection kits (without Exo□) served as their controls. Our result showed that the RPA-Exo□ and MIRA-Exo□ detection kits exhibited significant fluorescence signals over time compared with those of the RPA and MIRA kits **(Figure 5A)**. The distinct difference in fluorescence brightness between the Exo□-presence group (MIRA-Exo□ and RPA-Exo□) and Exo□-absence group (MIRA and RPA) can be directly visualized under LED UV blue light **(Figure 5B).** These results suggested that the ssDNA FQ reporter was cleaved by Exo□ contained in the commercial detection kit, and this type of FQ reporter was unsuitable for developing the Exo□-based detection.

Furthermore, to investigate the degradation degree of ssDNA caused by Exo□ in the detection kits, we tested a 5′ FAM-labelled ssDNA probe in these detection reactions. We found that 80% of the ssDNA probe added to the MIRA-Exo□ kits was digested to a 15-nt product (P1) **(Figure 5C and 5D)**, while in RPA-Exo□ kit, 50% and 40% of the ssDNA probe were degraded into a ~15-nt (P1) and ~5-nt (P2) in 20 min,

respectively, presenting a more intensified degradation than MIRA-Exo□ **(Figure 5C and 5E)**. It suggested Exo□ in the detection kits was capable of digesting the ssDNA probe or primer, leading to a low detection efficiency.

The different degrees of degradation between these two kinds of commercial kits might be caused by different amounts of T4 gp32 added, as T4 gp32 is a ssDNA-binding protein protecting the ssDNA from nuclease degradation [36]. To investigate whether the ssDNA-binding protein prevents ssDNA from Exo□ digestion, we incubated the ssDNA with two types of ssDNA-binding proteins (T4 gp32 or SSB) before Exo□ digestion. The ssDNA probe pre-incubated with 1 μl T4 gp32 (10 mg/ml), 1 μl or 5 μl SSB (1.58 mg/ml) showed no digested band compared to the control (0 μl) **(Figure 5F, 5G and 5H)**, which suggested the single-stranded DNA-binding protein was capable of protecting ssDNA from Exo□ digestion. These results indicated that adding more T4 gp32 could offset or minimize the effects of Exo□′ ssDNase activity in the commercial kits. The findings also suggested that ssDNA-binding proteins may regulate *in vivo* the degradation of ssDNA mediated by Exo□ in DNA repair or metabolism processes.

Key amino acid residues for ssDNase activity in ExoIII

To identify the key residues that determine the ssDNase activity of Exo□, we predicted the structure of Exo□-ssDNA by molecular docking. And the predicted residues (S217, R216, D214, W212, K176, R170, N153, K121, and Q112) **(Supplementary Figure S3A)** were expressed and purified for mutation analysis **(Figure 6A, Supplementary Figure S4A)**. Residues (W212, F213, K121, Y109, and D151) reported to play essential roles in the exonuclease and AP-endonuclease activities of Exo□ [4, 8] were also mutated for analysis. The result of the fluorescence monitoring assay on the FQ reporter indicated the mutants of S217A, R216A, K176A, or R170A displayed equal cleavage efficiency with wild type Exo□ on the FQ reporter; D214A, W212A, F213A, Y109A, N153A, and D151N produced no fluorescence signal; K121A or Q112A showed much weaker cleavage than the wild type **(Figure 6B)**. Meanwhile, gel electrophoresis on the digested products showed a consistent result with the fluorescence monitoring assay, but K121A exhibited undetectable digestion on the ssDNA probe **(Figure 6C and 6D)**. These results indicated the residues (D214, W212, F213, N153, D151, K121, and Y109) were crucial in the catalyzing of Exo□ on ssDNA. As six of these critical residues (W212, F213, N153, Y109, K121, and D151) have also been found to play critical roles in the dsDNA exonuclease and

AP-endonuclease activities of Exo□ (4), the ssDNase activity of Exo□ most likely shares the same active center with the other two enzymatic activities on dsDNA.

Among these mutants, K121A of Exo□ has been reported to have an AP-endonuclease activity on dsDNA [4]. With the weakened ssDNase activity demonstrated in our study, K121A can replace the wild type to be applied in the AP-endonuclease-based commercial kits with minimized effects of ssDNase activity. By comparing the digested products generated by S217A, R216A, K176A, R170A, Q112A, and wild type, we found that R170A produced a larger fragment than other mutants and wild type **(Figure 6E)**. It suggested that mutation of R170A affected the efficiency of Exo□ digestion on ssDNA. Based on the conservation indicator of all residues of Exo□ illustrated (https://consurfdb.tau.ac.il/index.php), these identified residues (W212, F213, D214, N153, Y109, K121, D151 and R170) were highly conserved among 300 homolog proteins **(Figure 6F and 6G)**. The structure of Exo□ is constructed as a four-layered sandwich, and its active center on dsDNA is located at the valley between the two inner layers [4, 5] **(Figure 6G)**.

R170A has an attenuated AP-endonuclease activity

The residue of R170 is located with the protruding structure α_M helix of Exo□, which helps Exo□ bind to dsDNA by stretching into the major groove [5]. To investigate if the mutation of R170A also affects the AP-endonuclease and exonuclease activities of Exo□ on dsDNA, we designed specific dsDNA substrates for the two types of activities. On the AP-endonuclease substrate, the mutation of R170 took a much longer time (10 min) to digest compared to the wild type (1 min) **(Supplementary Figure S5A and S5B)**, suggesting the mutation seriously impaired the efficiency of AP-endonuclease activity. The digestion process is described in **Supplementary Figure S5C**. On the exonuclease substrate, the mutant of R170A produced a much larger product than the wild type **(Supplementary Figure S5D and S5E)**. It might be because R170A retained the intact exonuclease activity on dsDNA but not on ssDNA, leading to a larger ssDNA intermediate compared to the wild type. The exonuclease activities of Exo□ on dsDNA and ssDNA involved in the digestion are described in **Supplementary Figure S5F**. Altogether, we deemed that R170 in the α_M helix structure may help recognize or stabilize the AP site on dsDNA or ssDNA substrate for further docking into the active site, and the mutation of R170 affects the AP-endonuclease and ssDNase activities of Exo□ but still retains its dsDNA exonuclease activity.

The proposed enzymatic action model of Exo□ on ssDNA

Since the ssDNase activity probably shares the same active center with its dsDNA-targeted activity, an appropriate ssDNA substrate for Exo□ should possess a 'V'-shaped micro-structure, similar to the ssDNA conformation in the B-formed dsDNA **(Figure 7A)**. According to the Exo□-ssDNA structure and the previously reported functions of the key residues [4], four primary functional units for enzymatic actions of Exo□ are defined: capturing unit (R170, at 3′ side of the cleavage site and three nucleotides away from it), phosphate-stabilizing unit (Y109, K121, and N153, at 5′ side of cleavage site and three nucleotides away from it), sugar ring-stacking unit (W212, F213, and D214) and phosphodiester-cleaving unit (D151), all of which also represent four sequential steps in the digestion process **(Figure 7B)**. Unit 1(R170), located at the surface of Exo□ and functioning at the 3′ side of the cleavage site, is most likely the first contact with the substrate, the involvement of which naturally drives the endonuclease action on ssDNA. In the endonuclease model, interactions of unit 1 and unit 2 with ssDNA substrates can help convert the ~6 nucleotides at 3′ end of ssDNA to form a 'V' shape intermediate, suitable for the following actions of unit 3 and unit 4. Certain ssDNA substrates, such as the consecutive identical bases (Figure 4), might have difficulty in converting to the necessary conformation, resulting in the inhibition of Exo□ digestion; Meanwhile, the substrates with "V" conformation internally possibly attract units 2 and 3 of Exo□ binding to the site and triggering the endonucleolytic digestion, which explains the products of endonuclease activity in the mass spectrometry analysis (Figure 3). In the exonuclease model, some types of ssDNA (possibly short ssDNA or others with suitable micro-structure) might directly enter the active center without contacting unit 1 and sequentially be processed by units 2, 3, and 4 **(Figure 7C)**.

Combining with the structure analysis and the digestion results of Figure 2 and 3, we proposed the enzymatic actions of Exo□ digestion on ssDNA: the ssDNA substrate tends to be captured by the outer-layered unit 1, then stabilized by the inter-layered units 2 and 3, finally cleaved by unit 4 of Exo□, producing short fragments of ssDNA (endonuclease activity). The short ssDNA (~3 nt) or others with suitable micro-structure might directly enter into the active center and be processed by unit 2, unit 3, and unit 4 into nucleotides (exonuclease activity) **(Figure 7D)**. The model reflects a distributive catalyzation of Exo□ on ssDNA. In summary, ssDNA substrate is likely to undergo fragmentation by the endonuclease activity of Exo□, and the resulting small fragments are subsequently digested by the exonuclease activity of Exo□ into mononucleotides. Without the base-pairing of complementary strands, the conformation of ssDNA is easily affected by ion concentration, interacted

protein, temperature, and other factors in the solution. All these elements together forge the specific catalytic pattern of Exo□ on ssDNA.

Exo□ digested the dsDNA structures containing 3′ end ssDNA

To explore the biological significance of the ssDNase activity of Exo□, we examined several dsDNA substrates containing ssDNA (dsDNA with 3′ ssDNA flap, dsDNA with 3′ protruding ssDNA tail, bubble and fork-shaped dsDNA) that might occur in the biological process. After being treated with Exo□, our result demonstrated that Exo□ was capable of digesting the dsDNA with a 3′ flap **(Figure 8A).** The 3′ flap-removing capability of Exo□ may originate from its ssDNase activity **(Figure 8B).** The analysis of the gray intensity indicated the dsDNA with 3′ flap was digested with time **(Figure 8C).** Based on our results and the gap creation ability of Exo□ previously reported [8], we proposed the novel biological role of Exo□ in DNA repair: when the 3′ flap occurs, Exo□ recognize and remove the ssDNA flap by the ssDNase activity; then it continues to digest the ssDNA on dsDNA and create a gap; the resulting intermediate recruits the DNA polymerase to re-synthesize the complementary strand and fill the ssDNA gap; finally, the nick left is sealed by DNA ligase **(Figure 8D)**.

We next tested its ability to cleave the dsDNA substrates with a protruding ssDNA (≥ 4 nt) at the 3′ end, previously reported as resistant to Exo□ digestion [12]. Our results on the dsDNA with a 10-base protruding structure indicated that Exo□ could rapidly digest the dsDNA with a 3′ end 10-base ssDNA tail **(Supplementary Figure S6A and S6B)**. But for the dsDNA with 4-base protruding ssDNA at the 3′ end, the digestion occurred at 10 min, suggesting the efficiency of digestion significantly decreased to about one-tenth of the 10-base protruding structure **(Supplementary Figure S6C and S6D)**. Unlike the previous study [12], our results demonstrated that Exo□ could catalyze dsDNA structure with 3′ end protruding bases (≥ 4 nt). Furthermore, we found when the 3′ end 4-base protruding ssDNA was replaced with four adenylates, the dsDNA showed no digestion over 10 min **(Supplementary Figure S6E and S6F)**, suggesting the 3′ A_4-protruding ssDNA was resistant to the ssDNase activity of Exo□ and protected the dsDNA duplex from Exo□ digestion. Therefore, dsDNA with 3′ A_4-protruding ssDNA can be used for related enzymatic research of Exo□ or as the aptamer of biosensors, as the previous typical substrate may not protect itself from being cleaved by the ssDNase activity and the following exonuclease of Exo□. Based on the structural analysis that indicated the α_M helix was exactly 4~5 nt apart from the AP site (located in the active center) **(Supplementary Figure S6G and S6H)**, we

speculated that the lower efficiency of digestion on the 4-base protruding dsDNA might be because the topology of dsDNA-ssDNA junction site was not well recognized by α_M helix, which was unfavourable for the ssDNA further docking into the active center.

The fork structure was slightly digested by Exo□ in the first minute and completely degraded over 10 min **(Supplementary Figure S7A)**. To test if the ssDNA binding protein affects the digestion of Exo□, the fork structure was incubated with T4 gp32 for 10 min before adding Exo□. The result indicated that 1 μl T4 gp32 (10 mg/mL) protected over 40% of the substrate from digestion, significantly higher than 0.2 μl (~10%) **(Supplementary Figure S7A)**. This protection effect suggested that Exo□ started the digestion of the structure from the 3′ end ssDNA, and the binding of T4 gp32 to the 3′ end ssDNA prevented the dsDNA from being digested **(Supplementary Figure S7B)**. The analysis on gray intensity showed Exo□ was able to digest the fork dsDNA structure and the single binding protein delayed the process by binding to the ssDNA part **(Supplementary Figure S7C and S7D)**. The bubble structure showed no apparent digestion over time **(Supplementary Figure S7E and 7F)**. Collectively, these results indicated Exo□ may function in more types of dsDNA structures with 3′ ssDNA in DNA-repair or -metabolism processes.

Discussion

Defining the ssDNase activity of Exo□ is crucial for understanding its biological roles and guiding the current diagnostic applications. In this study, we adopted the sensitive ssDNase indicator FQ reporters, a range of short ssDNA substrates (~20 nt), and mass spectrometry analysis for prudent confirmation and systematic characterization of the ssDNase activity of Exo□. Our results uncovered that Exo□ possessed highly efficient 3′→5′ exonuclease and endonuclease activities on ssDNA, with the cleavage site at the 5′ side bond of the phosphodiester. As the discovery may remould the roles of Exo□ in its industrialized application and biological understanding in the DNA repair process, we assessed its effects by testing the popular commercialized kits containing Exo□ and investigated its possible biological functions through the dsDNA structures containing ssDNA that might occur *in vivo*. Our results showed that Exo□ digested ssDNA probes or primer in the isothermal amplification kit and dsDNA structures containing 3′-end ssDNA. To minimize the effects of Exo□′ ssDNase activity, we advise: a) adding more single-strand DNA binding protein T4 gp32 protects the primer or ssDNA probe from degradation of Exo□ in the isothermal

amplification kits; b) adding four or more consecutive adenylates at the 3′-end of the dsDNA structure or ssDNA helps inhibit the degradation of Exo□; c) with limited ssDNase activity, K121A and R170A mutants can replace the wild type and be applied in the AP-endonuclease and exnuclease based diagnostics, respectively; d) raise the reaction temperature to ≥ 42□, as the ssDNase activity of Exo□ was found highly suppressed in the temperature range. Considering that the ssDNase activity of Exo□ shares the same active center as its dsDNA-targeted activity, examining its biological roles *in vivo* by individual point mutation seems challenging. But digesting the dsDNA with 3′ flap ssDNA or 3′ protruding ssDNA tail *in vitro* indicated the ssDNase activity of Exo□ may confer a 3′ flap-cleaving ability, suggesting it might be competent to deal with more types of DNA lesions. During this, the ssDNA-binding proteins may play a regulatory role in Exo□-related ssDNA degradation *in vivo*. As a multi-functional nuclease, the enzymatic activities of Exo□ identified so far are summarized in **Supplementary Table S3**.

The endonuclease activity of Exo□ on ssDNA was confirmed for the first time by mass spectrometry analysis on Probe 1 and Probe 2. It might explain why digested products of Exo□ and LbCas12a only accounted for 50%~80% of their deactivated counterparts (Figure 3C, 3G, and 3K). The lost 20~50% fluorescence is possibly caused by Exo□ or LbCas12a cleaving the substrates and forming products with different lengths, which travelled in the gel at different speeds, finally leading to being dispersed or invisible under UV light. Combining these results with the analysis of the constructed crystal structure of Exo□-ssDNA, we proposed a theoretical model for understanding the underlying mechanism of endonuclease and exonuclease actions of Exo□ on ssDNA. Steven A. Benner and his coworkers observed that Exo□ could bypass two consecutive nucleotides with phosphorothioate modification and continued deleting the ssDNA [21], which might be well-explained by endonuclease activity in the model. In addition, its human homolog APE1 has been reported to have a strong binding affinity to the G-rich oligo (5′-AGGGCGGTGTGGGAAGAGGGAAGAGGGGGAGG-3′, a 32-nt sequence of the oncogene KRAS promoter) [37]. Thus, Exo□ also possibly bound to the G-rich region of Probe 2 and activated its endonuclease activity, producing more middle fragments than the other two ssDNA probes, as indicated in mass spectrometry analysis.

Another interesting finding is that the consecutive identical bases of ssDNA stalled the digestion of Exo□. In the early 1960s, the inactivity of Exo□ on ssDNA was coined by Kornberg's laboratory based on an ssDNA oligo of five consecutive Ts (5′ pTpTpTpTpT 3′) [11] (which might not be sufficiently prudent to conclude that Exo□ is

inactive on all ssDNA). In 2007, Steven A. Benner and his coworkers pointed out for the first time that Exo□ could degrade ssDNA by incubating with two long ssDNA oligos (51 nt) [21]. An approximate 43-mer band occurred as the superior product when the concentration of Exo□ decreased, but the reason remains unclear. Here, based on our conclusion, the 43-mer intermediate exactly corresponds to the product generated when Exo□ stalled its digestion ahead of the consecutive GGG (Position 40-42) of the ssDNA substrate in 3′→5′ direction (5′-GCGTAATACGACTCACTATAGACGAGCGTACTTTAGTGA**GGG**TTAATT CGC-3′). In addition, adding 10 T bases to an ssDNA at the 3′ end has been indicated to suppress Exo□ digestion [18]; a *Saccharomyces cerevisiae* homolog of Exo□, CCR4 (an ssDNA exonuclease), has also been reported to have a slower degradation on the substrate with 3′ end five consecutive As and was unable to cleave when the ssDNA contained ten consecutive As within [38]. Based on our proposed model, the sequence feature of consecutive identical bases in ssDNA may create an unfavorable local microstructure that can impede Exo□ digestion.

Our work uncovers the long-underestimated ssDNase activity of Exo□, dissects the underlying enzymatic behaviors of Exo□ on ssDNA and advances the mechanism understanding of its biological roles in DNA repair. Future investigations might be conducted: 1) crystal structure of the Exo□-ssDNA complex (endonuclease and exonuclease model); 2) potential biological roles of the ssDNase activity *in vivo*. A better understanding of the underlying enzymatic actions of this multifunctional enzyme will facilitate efficient and reliable applications of Exo□-based nucleic acid diagnostics.

MATERIALS AND METHODS

Material and reagents

To avoid any potential secondary structure formed, we used short ssDNA oligos (5~23 nt) (Sunya Biotechnology Co., Hangzhou, Zhejiang Province, China) as the substrate for the nuclease treatment. The FQ reporter was a synthesized ssDNA oligo labelled with a fluorophore (FAM or FITC) at its 5′ end and a quencher (BHQ1) at its 3′ end. The FQ ssDNA reporter is a sensitive sensor of ssDNA-cleaving activity, enabling a fluorescence signal's visible emission upon ssDNase-like activity-mediated cleavage [26]. The other reporter (termed the FB reporter) was an ssDNA oligo labelled

with FAM at the 5′ end and biotin at the 3′ end, which is tailored for use in lateral flow strips and yields a positive result upon cleavage by ssDNase activity, as indicated by the appearance of two lines on the strip [26]. All the sequences and related modifications are detailed in **Supplementary Table S4**. Exo□ (NEB#M0206V), APE1 (NEB#M0282S), T7 exonuclease (T7 exo) (NEB#M0263L) and LbCas12a (NEB#M0653S) were bought from New England Biolabs (Ipswich, MA, USA). The solutions of $MgCl_2$ and EDTA-2Na (referred to as EDTA) (Sinopharm Chemical Reagent Co., Ltd. Shanghai, China) were respectively prepared with deionized water to concentrations of 10 mM (pH = 7) and 100 mM (pH = 8). The 5′ FAM-labelled ssDNA constructed with 5 nt, 15 nt, 20 nt, and 30 nt adenylates were synthesized and used as the ssDNA marker in the gel electrophoresis.

Protein expression and purification

The protein expression and purification followed the method in the previous study [4]. The wild type of Exo□ gene (*E. coli*) (GeneID:946254) and the DNA fragments of mutants (S217A, R216A, D214A, F213A, W212A, K176A, D151N, R170A, N153A, K121A, Q112A, Y109A) were cloned into pET-30a (6×His–Exo□) by using ClonExpress II One Step Cloning Kit (Vazyme Biotech, Nanjing, China). These vectors were transformed into Rosetta (DE3) *E. coli* (LGC Biosearch Technologies, Hoddesdon, UK). After the plasmids were confirmed by sequencing, cells were placed in a 37°C incubator (adding 100 μg/mL kanamycin) and shaken until the OD600 = 0.6. Then, the culture was added with 1 mM IPTG (final concentration) and incubated at 16°C shaking incubator for 16 hours. Cells were collected by centrifugation at 7500 × g for 10 min and resuspended in 20 mL PBS buffer (137 mM NaCl, 2.7 mM KCl, 10 mM Na_2HPO_4, and 1.8 mM KH_2PO_4, pH=7.8). The suspensions were sonicated with 4 s pulse-on and 6 s pulse-off (P = 150W) for 15~30 min. Products were centrifuged at 15000 × g for 15 min, and then the supernatants were retained and filtered by micro syringe filters (0.45 μm). The protein was purified with HisSep Ni-NTA 6FF Chromatography Column (Yeasen Biotechnology Co., Ltd., Shanghai, China). After dialysis in PBS buffer, these proteins were aliquoted with 20% glycerol and stored at -80°C. The tag does not affect the enzymatic activity of Exo□ [4] **(Supplementary Figure S3).**

Fluorescence monitoring assay on FQ reporter

In the assay, 5 μM ssDNA FQ reporter was incubated with Exo□ (5 U/μl), T7 exo (5 U/μl), APE1 (5 U/μl) or LbCas12a-crRNA-activator complex (0.1 μM). To form the LbCas12a-crRNA-activator complex, LbCas12a crRNA and the activator dsDNA

are pre-incubated at 37°C for 10 min before incubating with FQ reporter. The corresponding buffer for each nuclease was added based on the manufacturer's document, and the total reaction volume was supplemented to 10 μl by the nuclease-free water. During the incubation, the fluorescence value was recorded every minute for over 30~60 min at 37°C by Mx3500P (Agilent, CA, USA). The endpoint detection here was defined as detecting the accumulated fluorescence once at the end of the reaction. The image of fluorescence excited by LED blue light was captured in an Ultra Slim LED illuminator (Miulab, Hangzhou, Zhejiang Province, China).

Enzymatic reaction on ssDNA

The enzymatic reaction contained 5 μM fluorophore-labelled ssDNA oligos, 5 U/μl commercial Exo□ or 2.5 μM purified wildtype and mutant Exo□, 1 μl 10x NEbuffer #1. The total reaction volume was supplemented to 10 μl by nuclease-free water. Before being treated with T7 exonuclease (T7 exo) (5 U/μl), APE1 (5 U/μl), Exo□ or LbCas12a-crRNA-activator complex (0.1 μM), the ssDNA oligos were incubated at 95°C for 5 min, then cooled down in the ice. The nucleases were deactivated by heat at 95°C for 5 min and used as controls (D-T7 exo, D-APE1, D-Exo□, and D-LbCas12a). After incubating in a 37°C water bath for 40 min, enzymatic reaction products were subjected to gel electrophoresis.

Different dsDNA substrates were prepared to investigate the roles of Exo□ in DNA repair. An equivalent amount of complementary ssDNAs (10 μM) was mixed and annealed to each other by heating at 95°C for 5 min and cooling down at room temperature for 30 min. The generated dsDNA (5 μM) was incubated with Exo□ (2.5 μM), and the reaction product was then analyzed by gel electrophoresis.

The trans-cleavage reaction of LbCas12a on ssDNA

For the reaction of LbCas12a on ssDNA, crRNA and dsDNA activators for the trans-cleavage activity of LbCas12a were prepared. The crRNA was synthesized using the T7 *in vitro* transcription kit (Vazyme Biotech, Nanjing, China). The dsDNA template for transcription was designed by annealing a single-stranded DNA (ssDNA) comprising T7 promotor and crRNA sequence (SUNYA Biotechnology Co., Ltd, Zhejiang, China) to its complementary oligonucleotides. A total volume of 20 μl was prepared by mixing template dsDNA (~100 ng), 2 μl of T7 RNA polymerase, 8 μl of NTP buffer, 2 μl of reaction buffer, and nuclease-free water. The reaction mix was incubated at 37°C water bath for 16 h. The transcription product was treated with TURBO™ DNase (Thermo Fisher Scientific, Massachusetts, USA) at 37°C for 30

min and purified by Monarch RNA Cleanup Kit (New England Biolabs, Massachusetts, USA). The concentration of crRNA was determined by Nanodrop 2000 (Thermo Fisher Scientific, Massachusetts, USA). The dsDNA activator for the trans-cleavage activity of LbCas12a was created by annealing complementary ssDNAs containing PAM and the target sequence against crRNA. To form the LbCas12a-crRNA-activator complex, LbCas12a crRNA, and the activator dsDNA are pre-incubated at 37°C for 10 min before incubating with an ssDNA probe or FQ reporter. The sequences are presented (**Supplementary Table S4)**.

The fluorescence-based gel electrophoresis assay

The gel was prepared with a concentration of 6% (wt/vol) agarose (HydraGene Co., Ltd, Xiamen, Fujian Province, China). After incubating with Exo□, the reaction mixtures mixed with a 6×loading buffer (Takara, Beijing, China) were loaded into the gel. The electrophoresis (EPS300, Tanon, Shanghai, China) was carried out at 130 V for ~40 min in Tris-acetate-EDTA (TAE) running buffer (400 mM Tris, 25 mM EDTA, adding acetic acid to pH =7.8). A dark environment was required during electrophoresis to slow down fluorescence extinction. The abundance of reaction products was indicated by fluorescence bands under UV light, which was visualized and imaged by a multifunctional ultra-sensitive imaging system (Shenhua Science Technology Co. Ltd., Hangzhou, Zhejiang Province, China).

Mass spectrometry analysis

After 5 μM fluorophore-labelled ssDNA oligo was incubated with 5 U/μl Exo□ at 37°C for 0.5 h, the enzymatic reaction was stopped by heating at 95°C for 5min. The reaction product was then analyzed by mass spectrometry. The reaction containing only ssDNA oligo or Exo□ was prepared as the control. Before incubation at 37°C, the ssDNA oligos were pre-incubated at 95°C for 5 min and cooled in the ice. Hippo Biotechnology Co., Ltd. performed the mass spectrometry (Thermo LTQ-XL, Massachusetts, USA) analysis on the samples (Huzhou, Zhejiang, China). The detection range of molecular weight in mass spectrometry is 500~20000 Da. Electron Spray Ionization (ESI) was used to ionize the molecules.

Molecular docking

Molecular docking of Exo□ (PDB code: 1AKO) and ssDNA (NDB ID: 1S40) was performed in a webserver (https://wenmr.science.uu.nl/haddock2.4/)[39-41]. Before the docking, we performed structure alignment or superimposing on Exo□ and

APE1-dsDNA (PDB ID: 1DE8 and NDB ID: 5WN5) complex through TM-align (Version 20190822) (https://zhanggroup.org/TM-align/)[42]. We extracted the structure of the Exo□-ssDNA complex by PyMOL[43] **(Supplementary Figure S7)**. Residues of Exo□ located within 5 Å of the ssDNA and the last four nucleotides at the 3′ end of the ssDNA were selected to input in the HADDOCK website for molecular docking. Docking parameters were set by default. The output structure of Exo□-ssDNA with the highest score was visualized by PyMOL for further analysis.

Evaluation of the Exo□′ ssDNase activity in the commercial diagnostic kits

To examine the effects of Exo□′ ssDNase activity on the commercial isothermal amplification detection kit containing Exo□, we tested four kits including RPA (recombinase polymerase amplification) with Exo□ (TwistAmp® exo) or without Exo□ (TwistAmp® Basic) (Abbott, Illinois, US), MIRA (Multienzyme Isothermal Rapid Amplification) with (Fluorescence type) or without Exo□ (Basic type) (Amplification Future company, Weifang, Shandong Province, China) by FQ reporter and 5′-FAM-labelled ssDNA probe. All the reagents were added to the lyophilized powder following the usage instructions. Then 5 μl ssDNA FQ reporter or probe (10 μM) was added to the reaction mix. The tubes containing the reaction mixture were incubated in Mx3500P (Agilent, Santa Clara, CA, USA) at 37°C for 30 min to monitor the fluorescence generated. The endpoint fluorescence was visualized under an LED blue light transilluminator (THBC-470) (TUOHE ELECTROMECHANICAL TECHNOLOGY CO., LTD, Shanghai, China).

Data availability

The data underlying this article are available from the corresponding author upon request.

References

1 Robertson AB, Klungland A, Rognes T, Leiros I. DNA repair in mammalian cells: Base excision repair: the long and short of it. *Cell Mol Life Sci* 2009; **66**:981-993.

2 van der Veen S, Tang CM. The BER necessities: the repair of DNA damage in human-adapted bacterial pathogens. *Nat Rev Microbiol* 2015; **13**:83-94.

3 Lovett ST. The DNA Exonucleases of Escherichia coli. *EcoSal Plus* 2011; **4**.

4 Lee D, Oh S, Cho H, Yoo J, Lee G. Mechanistic decoupling of exonuclease III

multifunctionality into AP endonuclease and exonuclease activities at the single-residue level. *Nucleic Acids Res* 2022; **50**:2211-2222.

5 Mol CD, Kuo CF, Thayer MM, Cunningham RP, Tainer JA. Structure and function of the multifunctional DNA-repair enzyme exonuclease III. *Nature* 1995; **374**:381-386.

6 Centore RC, Lestini R, Sandler SJ. XthA (Exonuclease III) regulates loading of RecA onto DNA substrates in log phase Escherichia coli cells. *Mol Microbiol* 2008; **67**:88-101.

7 Rogers SG, Weiss B. Exonuclease III of Escherichia coli K-12, an AP endonuclease. *Methods Enzymol* 1980; **65**:201-211.

8 Yoo J, Lee D, Im H *et al*. The mechanism of gap creation by a multifunctional nuclease during base excision repair. *Sci Adv* 2021; **7**.

9 Biertumpfel C, Zhao Y, Kondo Y *et al*. Structure and mechanism of human DNA polymerase eta. *Nature* 2010; **465**:1044-1048.

10 Richardson CC, Kornberg A. A Deoxyribonucleic Acid Phosphatase-Exonuclease from Escherichia Coli. I. Purification of the Enzyme and Characterization of the Phosphatase Activity. *J Biol Chem* 1964; **239**:242-250.

11 Richardson CC, Lehman IR, Kornberg A. A Deoxyribonucleic Acid Phosphatase-Exonuclease from Escherichia Coli. Ii. Characterization of the Exonuclease Activity. *J Biol Chem* 1964; **239**:251-258.

12 Henikoff S. Unidirectional digestion with exonuclease III creates targeted breakpoints for DNA sequencing. *Gene* 1984; **28**:351-359.

13 Hoheisel JD. On the activities of Escherichia coli exonuclease III. *Anal Biochem* 1993; **209**:238-246.

14 Smith AJ. The use of exonuclease III for preparing single stranded DNA for use as a template in the chain terminator sequencing method. *Nucleic Acids Res* 1979; **6**:831-848.

15 Liu H, You Y, Zhu Y, Zheng H. Recent advances in the exonuclease III-assisted target signal amplification strategy for nucleic acid detection. *Anal Methods* 2021; **13**:5103-5119.

16 Stringer OW, Andrews JM, Greetham HL, Forrest MS. TwistAmp® Liquid: a versatile amplification method to replace PCR. *Nature Methods* 2018; **15**:395-395.

17 Piepenburg O, Williams CH, Stemple DL, Armes NA. DNA detection using recombination proteins. *PLoS Biol* 2006; **4**:e204.

18 Cai Z, Chen Y, Lin C *et al*. A dual-signal amplification method for the DNA detection based on exonuclease III. *Biosens Bioelectron* 2014; **61**:370-373.

19 Xu Q, Cao A, Zhang LF, Zhang CY. Rapid and label-free monitoring of

exonuclease III-assisted target recycling amplification. *Anal Chem* 2012; **84**:10845-10851.

20 Shen Y, Yuan H, Guo Z, Li XQ, Yang Z, Zong C. Exonuclease III Can Efficiently Cleave Linear Single-Stranded DNA: Reshaping Its Experimental Applications in Biosensors. *Biosensors (Basel)* 2023; **13**.

21 Yang Z, Sismour AM, Benner SA. Nucleoside alpha-thiotriphosphates, polymerases and the exonuclease III analysis of oligonucleotides containing phosphorothioate linkages. *Nucleic Acids Res* 2007; **35**:3118-3127.

22 Shevelev IV, Hubscher U. The 3 '-5 ' exonucleases. *Nature Reviews Molecular Cell Biology* 2002; **3**:364-375.

23 Matyus L, Szollosi J, Jenei A. Steady-state fluorescence quenching applications for studying protein structure and dynamics. *J Photochem Photobiol B* 2006; **83**:223-236.

24 Zhuang X, Ha T, Kim HD, Centner T, Labeit S, Chu S. Fluorescence quenching: A tool for single-molecule protein-folding study. *Proc Natl Acad Sci U S A* 2000; **97**:14241-14244.

25 Kasry A, Ardakani AA, Tulevski GS, Menges B, Copel M, Vyklicky L. Highly Efficient Fluorescence Quenching with Graphene. *The Journal of Physical Chemistry C* 2012; **116**:2858-2862.

26 Kaminski MM, Abudayyeh OO, Gootenberg JS, Zhang F, Collins JJ. CRISPR-based diagnostics. *Nat Biomed Eng* 2021; **5**:643-656.

27 Wang H, Li H, Tang B *et al.* Fast and sensitive differential diagnosis of pseudorabies virus-infected versus pseudorabies virus-vaccinated swine using CRISPR-Cas12a. *Microbiol Spectr* 2024; **12**:e0261723.

28 Chen JS, Ma E, Harrington LB *et al.* CRISPR-Cas12a target binding unleashes indiscriminate single-stranded DNase activity. *Science* 2018; **360**:436-439.

29 Gootenberg JS, Abudayyeh OO, Lee JW *et al.* Nucleic acid detection with CRISPR-Cas13a/C2c2. *Science* 2017; **356**:438-442.

30 Mitsunobu H, Zhu B, Lee SJ, Tabor S, Richardson CC. Flap endonuclease activity of gene 6 exonuclease of bacteriophage T7. *J Biol Chem* 2014; **289**:5860-5875.

31 Daher RK, Stewart G, Boissinot M, Bergeron MG. Recombinase Polymerase Amplification for Diagnostic Applications. *Clin Chem* 2016; **62**:947-958.

32 Shen XX, Qiu FZ, Shen LP *et al.* A rapid and sensitive recombinase aided amplification assay to detect hepatitis B virus without DNA extraction. *BMC Infect Dis* 2019; **19**:229.

33 Lu S, Tong X, Han Y *et al.* Fast and sensitive detection of SARS-CoV-2 RNA using suboptimal protospacer adjacent motifs for Cas12a. *Nat Biomed Eng* 2022; **6**:286-297.

34 Zhi S, Shen J, Li X *et al*. Development of Recombinase-Aided Amplification (RAA)-Exo-Probe and RAA-CRISPR/Cas12a Assays for Rapid Detection of Campylobacter jejuni in Food Samples. *J Agric Food Chem* 2022; **70**:9557-9566.

35 Zhou S, Zheng X, Yang Z *et al*. Development of Two Recombinase Polymerase Amplification EXO (RPA-EXO) and Lateral Flow Dipstick (RPA-LFD) Techniques for the Rapid Visual Detection of Aeromonas salmonicida. *Mar Biotechnol (NY)* 2022; **24**:1094-1109.

36 Jensen DE, von Hippel PH. DNA "melting" proteins. I. Effects of bovine pancreatic ribonuclease binding on the conformation and stability of DNA. *Journal of Biological Chemistry* 1976; **251**:7198-7214.

37 Pramanik S, Chen Y, Song H *et al*. The human AP-endonuclease 1 (APE1) is a DNA G-quadruplex structure binding protein and regulates KRAS expression in pancreatic ductal adenocarcinoma cells. *Nucleic Acids Res* 2022; **50**:3394-3412.

38 Chen J, Chiang YC, Denis CL. CCR4, a 3'-5' poly(A) RNA and ssDNA exonuclease, is the catalytic component of the cytoplasmic deadenylase. *EMBO J* 2002; **21**:1414-1426.

39 Honorato RV, Koukos PI, Jimenez-Garcia B *et al*. Structural Biology in the Clouds: The WeNMR-EOSC Ecosystem. *Front Mol Biosci* 2021; **8**:729513.

40 van Zundert GCP, Rodrigues J, Trellet M *et al.* The HADDOCK2.2 Web Server: User-Friendly Integrative Modeling of Biomolecular Complexes. *J Mol Biol* 2016; **428**:720-725.

41 de Vries SJ, van Dijk M, Bonvin AM. The HADDOCK web server for data-driven biomolecular docking. *Nat Protoc* 2010; **5**:883-897.

42 Zhang Y, Skolnick J. TM-align: a protein structure alignment algorithm based on the TM-score. *Nucleic Acids Res* 2005; **33**:2302-2309.

43 Delano WL. The PyMOL Molecular Graphics System, DeLano Scientific, San Carlos, CA. 2002.

Acknowledgements

This work was supported by the Zhejiang Provincial Key R&D Program (2023C03045 & 2021C02008), the National Program on Key Research Project of China (2022YFC2604201 & 2019YFE0103900) as well as the European Union's Horizon 2020 Research and Innovation Programme under Grant Agreement No. 861917-SAFFI, Zhejiang Provincial Natural Science Foundation of China (LZ24C180002), Scientific Research Fund of Zhejiang Provincial Education Department (Y202250872), and Key Research and Development Program of Hangzhou (202203A08).

Contributions

H.W. performed the majority of experiments and wrote the manuscript; C.Y., Q.L., Z.J. and N.L. helped with electrophoresis experiments, protein purification and figure preparation; C.J., C.Z., C.Z., and G.Z. helped with the data analysis and offered technical support; M.Y. and Y.L. acquired funding and supervised the research; all authors discussed the results and commented on the manuscript.

Conflict of Interest

The authors declare no competing interests.

Figure legends

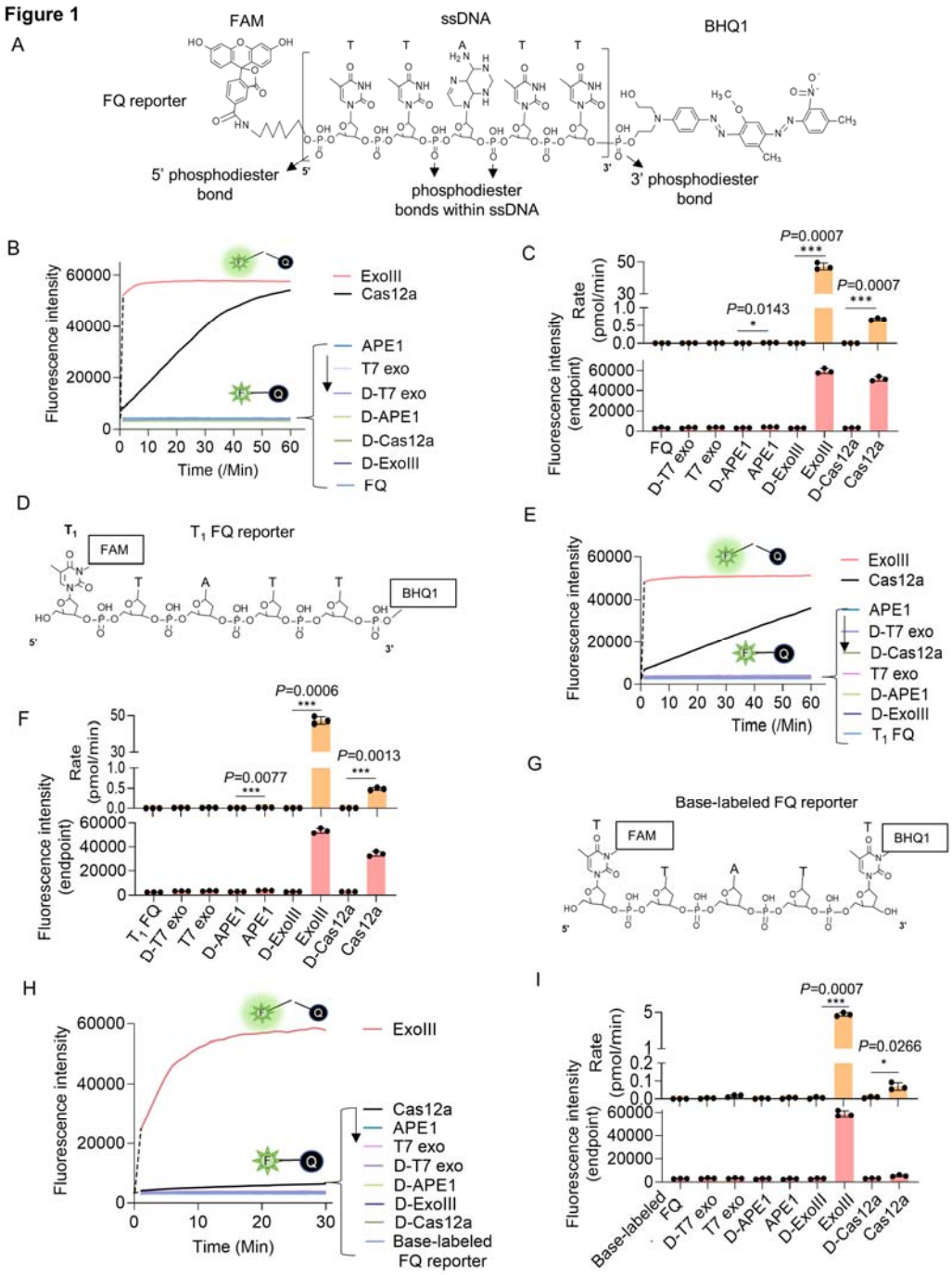

Figure 1. Exo□ (5 U/μl) rapidly cleaved the ssDNA FQ reporter (5 μM) of the CRISPR/Cas12a system with an average rate of 4.5~45 pmol ($2.7\sim27\times10^{12}$) phosphodiester bonds per minute. **(A)** The typical structure of the ssDNA FQ is presented, in which three types of putative susceptible sites for Exo□ digestion are outlined, including 5′ phosphodiester bond, phosphodiester bonds within ssDNA, and 3′

phosphodiester bond. **(B)** The fluorescence intensity of FQ reporter (5 μM) treated with four active nucleases (T7 exonuclease (T7 exo) (5 U/μl), APE1 (5 U/μl), Exo□ (5 U/μl), and Cas12a/crRNA (0.1 μM)) or their heat-deactivated counterparts (D-T7 exo, D-APE1, D-Exo□, D-Cas12a) was monitored every minute for 60 min. The dsDNA nuclease T7 exo was a negative control, also used to examine if the ssDNA substrates in the reaction formed dsDNA regions internally and between ssDNA strands, while LbCas12a with a trans-cleavage activity on ssDNA was a positive control. The D-nuclease served as the internal control of each active nuclease. The curve was plotted with an average value of three repeats. **(C)** The average rate of Exo□ digestion on FQ reporter was calculated by the formula: (the fluorescence produced/total fluorescence× 50 pmol)/reaction time. The total fluorescence means the fluorescence intensity generated when the input FQ reporter (50 pmol) was all cleaved. *P* (APE1 vs. D-APE1) = 0.0143; *P* (Exo□ vs. D-Exo□) = 0.0007; *P* (Cas12a vs. D-Cas12a) = 0.0007. **P*<0.05, and ****P*<0.001. The fluorescence intensity at the endpoint of the reaction was plotted based on three repeats, after the FQ reporter respectively treated with four active nucleases and their heat-deactivated counterpart (D-nuclease). **(D)** The 5′ T_1 FAM-labelled FQ reporter structure is designed and presented, in which the 5′ phosphodiester bond is removed and 3′ phosphodiester bond retained. **(E)** Real-time monitoring on the fluorescence generated upon 5′ T_1 FAM-labelled FQ reporter (5 μM) treated with four nucleases (T7 exonuclease (T7 exo) (5 U/μl), APE1 (5 U/μl), Exo□ (5 U/μl), and Cas12a-crRNA (0.1 μM)) or deactivated nucleases (D-T7 exo, D-APE1, D-Exo□, D-Cas12a) was performed for 60 min. The average value of four repeats was calculated and curved. **(F)** The average rate of Exo□ digestion on T_1-labelled FQ reporter was calculated by the formula: (the fluorescence produced/total fluorescence× 50 pmol)/reaction time. After the FQ reporter was treated with the four nucleases or their deactivated ones, the fluorescence intensities at the reaction endpoint were measured and plotted. *P* (APE1 vs. D-APE1) = 0.0077; *P* (Exo□ vs. D-Exo□) = 0.0007; *P* (Cas12a vs. D-Cas12a) = 0.0013. **(G)** The structure of the base-labelled FQ reporter for Exo□ is diagrammed, in which both 5′ and 3′ phosphodiester bonds are removed. **(H)** The digestion of the four nucleases and their deactivated counterparts on the base-labelled FQ reporter was monitored for 30 min. The average value of three repeats was calculated and curved. **(I)** The average rate of Exo□ digestion on the base-labelled FQ reporter was calculated by the formula: (the fluorescence produced/total fluorescence× 50 pmol)/reaction time. After the cleavage reactions on the FQ reporter, the fluorescence intensities at the reaction endpoint were measured and plotted. *P* (Exo□ vs. D-Exo□) =0.000006; *P* (Cas12a vs. D-Cas12a) =0.0185. The statistical analysis was performed using a two-tailed *t*-test.

*P<0.05, ***P<0.001. The dashed line in the figure does not indicate the real-time fluorescence generated in the reaction but only represents a trend in the period for monitor machine to initiate (~2 minutes).

Figure 2

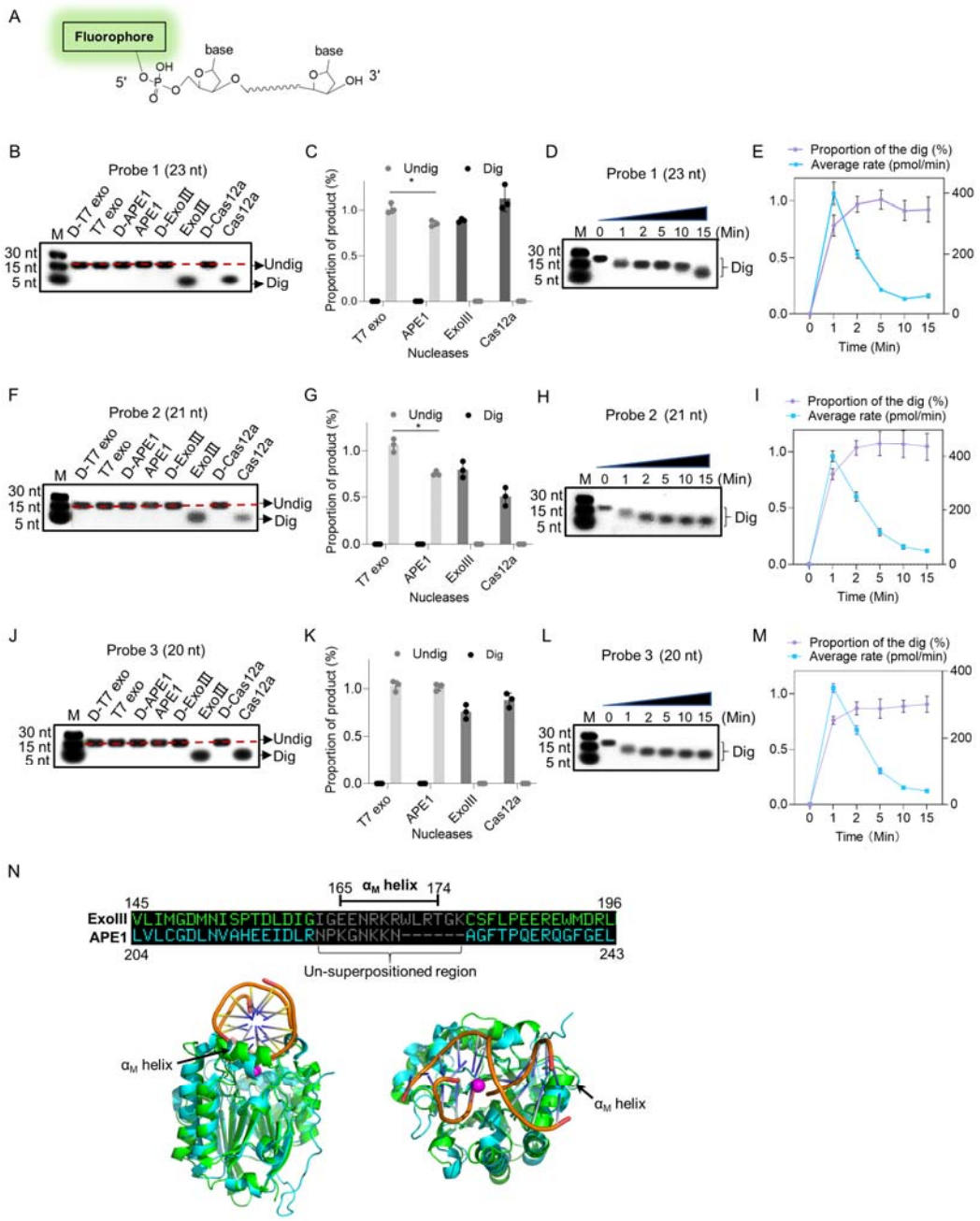

Figure 2. Exo□ (5 U/μl) digested the 5′ end fluorophore-labelled ssDNA substrates (5 μM) in a 3′ to 5′-end direction with a estimated rate of ~10^{13} nucleotides per minute. **(A)** The 5′ fluorophore-labelled ssDNA structure for the following Exo□ digestion is

shown. The squiggle line represents the ~20 nucleotides of the ssDNA oligo. **(B, F, and J)** The ssDNA oligo of Probe 1, Probe 2, or Probe 3 (5 μM) was treated with the four nucleases (T7 exo (5 U/μl), APE1 (5 U/μl), Exo□ (5 U/μl), and Cas12a-crRNA (0.1 μM)) and their deactivate counterpart (D-T7 exo, D-APE1, D-Exo□, D-Cas12a) for 30 min. The reaction products were analyzed by gel electrophoresis. Undig, undigested; dig, digested; M, maker. **(C, G, and K)** The gray intensity of the digested or undigested bands produced by the three probes was measured by ImageJ. The undigested or digested proportions were calculated with the formula: Proportion = (Intensity of the undigested or digested band produced in the active nuclease treatment)/(Intensity of the undigested band produced in the corresponding deactivated nuclease treatment)). *P* (APE1 vs. T7 exo on Probe 1) = 0.04; *P* (APE1 vs. T7 exo on Probe 2) = 0.02; **P*<0.05. The statistical analysis was performed using a two-tailed *t*-test. **(D, H, and L)** The time course of Exo□ digestion on the three probes was analyzed by gel electrophoresis, and the gray intensity of the generated bands was measured by ImageJ. **(E, I, and M)** The digesting rate of Exo□ on the ssDNA was calculated by: the digested proportion× 50 pmol × digested nucleotides/reaction time**.** The digested proportion was calculated by the formula: (gray intensity of the digested band produced)/(gray intensity of the band at 0 s)). Detailed information on these oligos is described in **Supplementary Table 4**. All experiments were repeated three times, and the representative ones were shown. **(N)** The structure alignment between Exo□ (PDB ID:1AKO) and APE1-dsDNA (PDB ID: 1DE8 and NDB ID: 5WN5) was performed by Pymol, and the un-superpositioned region (Residues 165-174, α_M helix) in the enzyme-substrate binding surface between Exo□ and APE1 was displayed. The aligned structures were shown from different angles by Pymol.

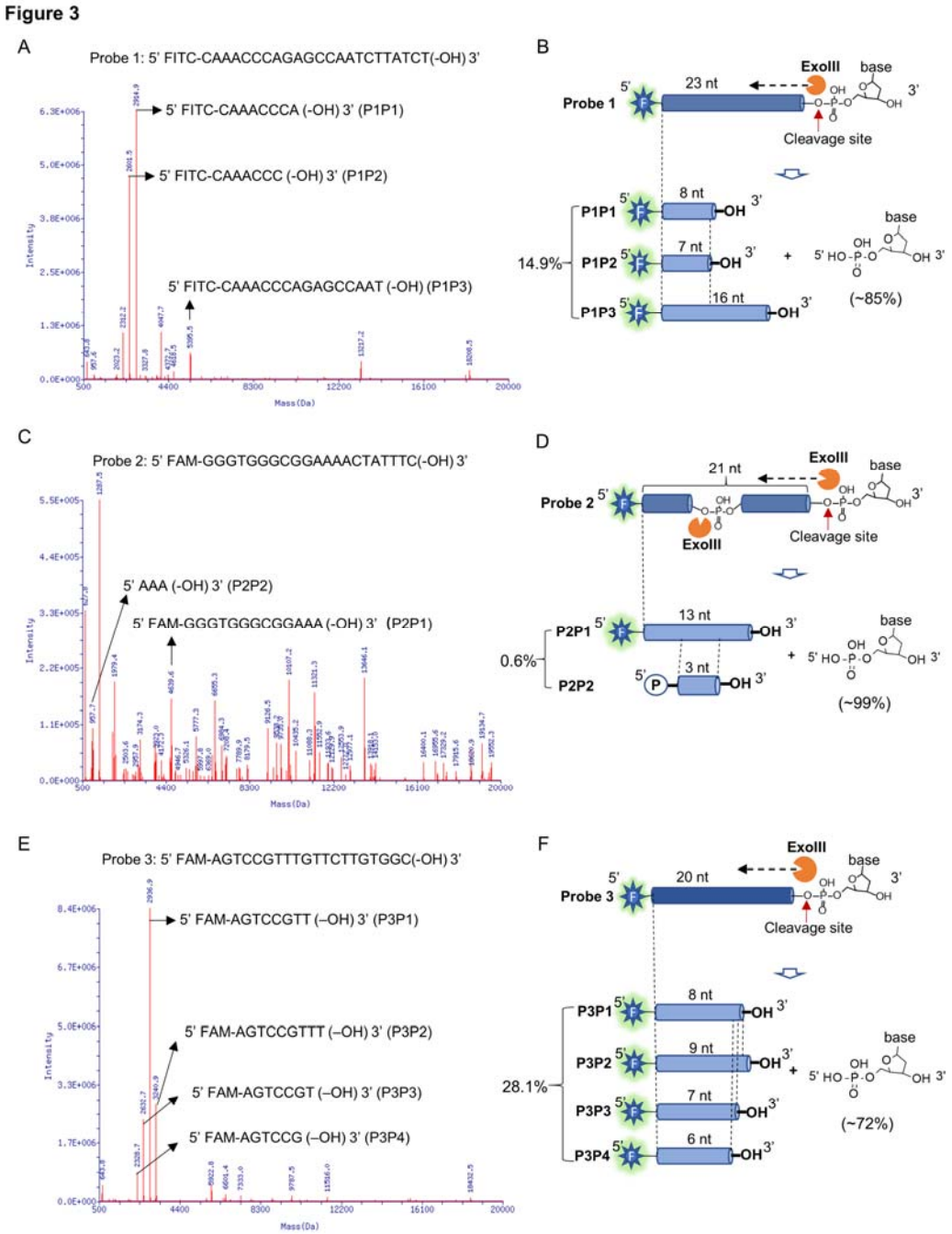

Figure 3. Mass spectrometry analysis revealed the exonuclease and endonuclease activities of Exo□ on ssDNA. After the ssDNA probe (5 μM) was incubated with Exo□ (5 U/μl) at 37°C for 30 min, the reaction product was analyzed by mass spectrometry. The detection range of mass spectrometry is 500~20000 Da. **(A)** The mass peaks of ssDNA Probe 1 digested by Exo□ are present. The three major peaks of reaction products of Probe 1 (P1P1, P1P2 and P1P3) are indicated by arrows. The information

related to major peaks is provided in Supplementary Table S1. **(B)** The digestion process, including the cleavage site, product and relevant proportion of Probe 1 is illuminated based on the mass spectrometry analysis. The three major mass peaks match three fragments of Probe 1 (8 nt, 7 nt and 16 nt), respectively. **(C)** The mass peaks of ssDNA Probe 2 digested by Exo□ are displayed. The two major peaks (P2P1 and P2P2) are labelled by arrows. **(D)** The digestion process of Probe 2 is illuminated based on the mass spectra analysis. The two major mass peaks of reaction products match two fragments of Probe 2 (13 nt and 3 nt). **(E)** The mass peaks of Probe 3 digested by Exo□ are displayed. The major peaks (P3P1, P3P2, P3P3, and P3P4) are labelled by arrows. **(F)** The reaction process of Probe 3 is illuminated based on the mass spectra analysis and gel result (Figure 3L). The four major mass peaks of reaction products match the fragments of Probe 3 (8 nt, 9 nt, 7 nt, and 6 nt). As the control, the mass peaks of undigested ssDNA probes are displayed in **Supplementary Figure S1**.

Figure 4

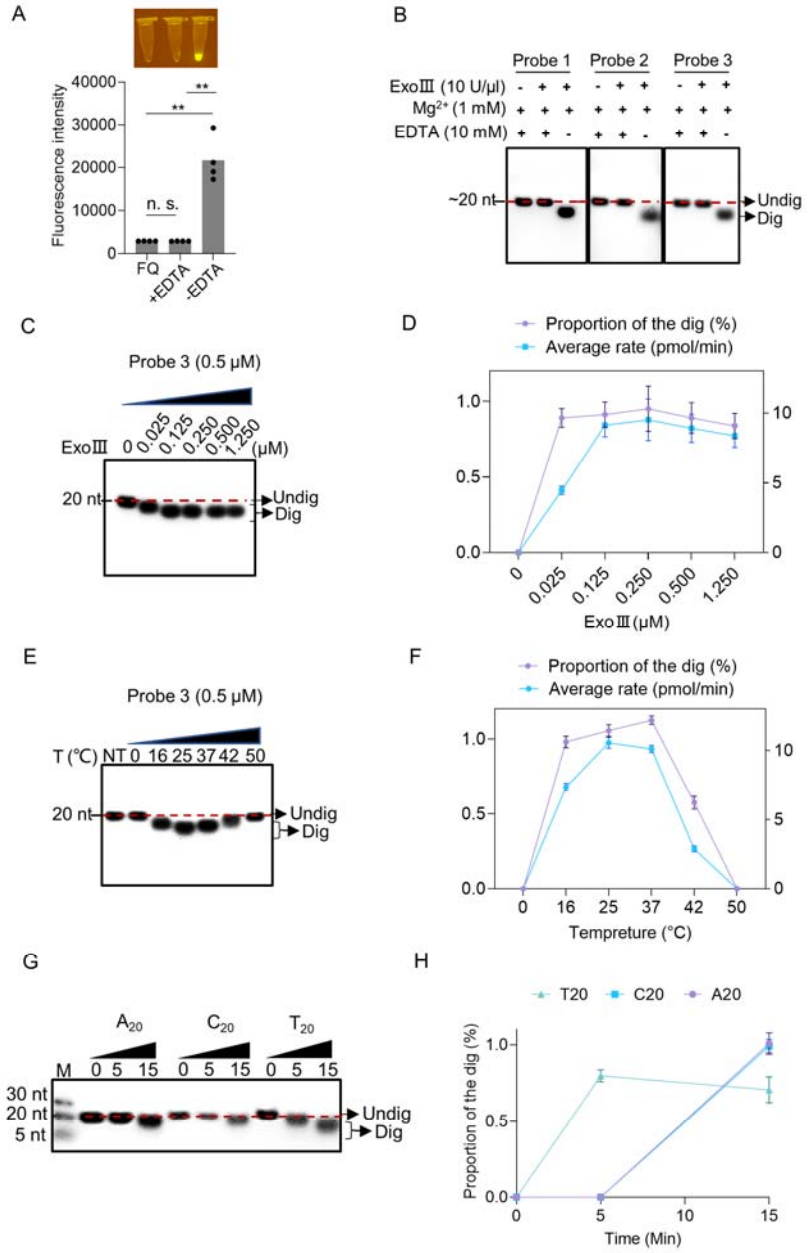

Figure 4. Enzymatic reaction conditions for the ssDNase activity of Exo□ were investigated. **(A)** EDTA (10 mM) was added with the mixture of FQ reporter (2.5 μM) and $MgCl_2$ (1 mM) before incubating with commercial Exo□ (5 U/μl) for 10 min. The fluorescence intensity generated in 10 min was measured and plotted on four repeats. The corresponding fluorescent tubes at the reaction endpoint were captured under LED UV light. The reaction without adding EDTA was regarded as a control. **P<0.01. The n.s. indicates no significance. Statistical significance was determined by a two-tailed *t*-test. **(B)** Three ssDNA probes (5 μM) with or without adding EDTA

were digested by commercial Exo□ (5 U/μl) for 10 min, and the reaction products were analyzed by gel. **(C)** Different amounts of purified Exo□ (0, 0.025, 0.125, 0.250, 0.500, and 1.250 μM) were incubated with ssDNA Probe 1 (0.5 μM) for 10 min, and the reaction products were analyzed by gel electrophoresis. **(D)** The digesting rate of Exo□ on the ssDNA was calculated by: the digested proportion× 50 pmol × digested nucleotides/reaction time. The digested proportion of Probe 3 was calculated by: (Gray intensity of the digested band)/(Gray intensity of the undigested band with 0 μM Exo□). **(E)** The ssDNA substrate (0.5 μM) was incubated with Exo□ (0.5 μM) at different temperatures (0, 16, 25, 37, 42, and 50°C) for 10 min, and the products were analyzed by gel electrophoresis. NT, no treatment. **(F)** The digested proportion of Probe 3 was calculated by: (Gray intensity of the digested band)/(Gray intensity of the undigested band (NT). **(G)** The 5′ FAM-labelled ssDNA probes constructed by 20 consecutive identical bases (A_{20}, C_{20}, T_{20}) were digested by Exo□ over 15 min, and the reaction products were separated by gel electrophoresis. The fluorescence intensity difference between the three oligos is caused by the bases covalently linked with a fluorophore. G_{20} was not tested here as it easily forms a G-quadruplex structure. **(H)** The gray intensity was determined by ImageJ. A digested proportion curve over 15 min was plotted from three repeats. The digested proportion was calculated by the formula: (Intensity of the digested band produced)/(Intensity of the band at 0 s). Data represents the average value of three repeats and is expressed as mean ± SD.

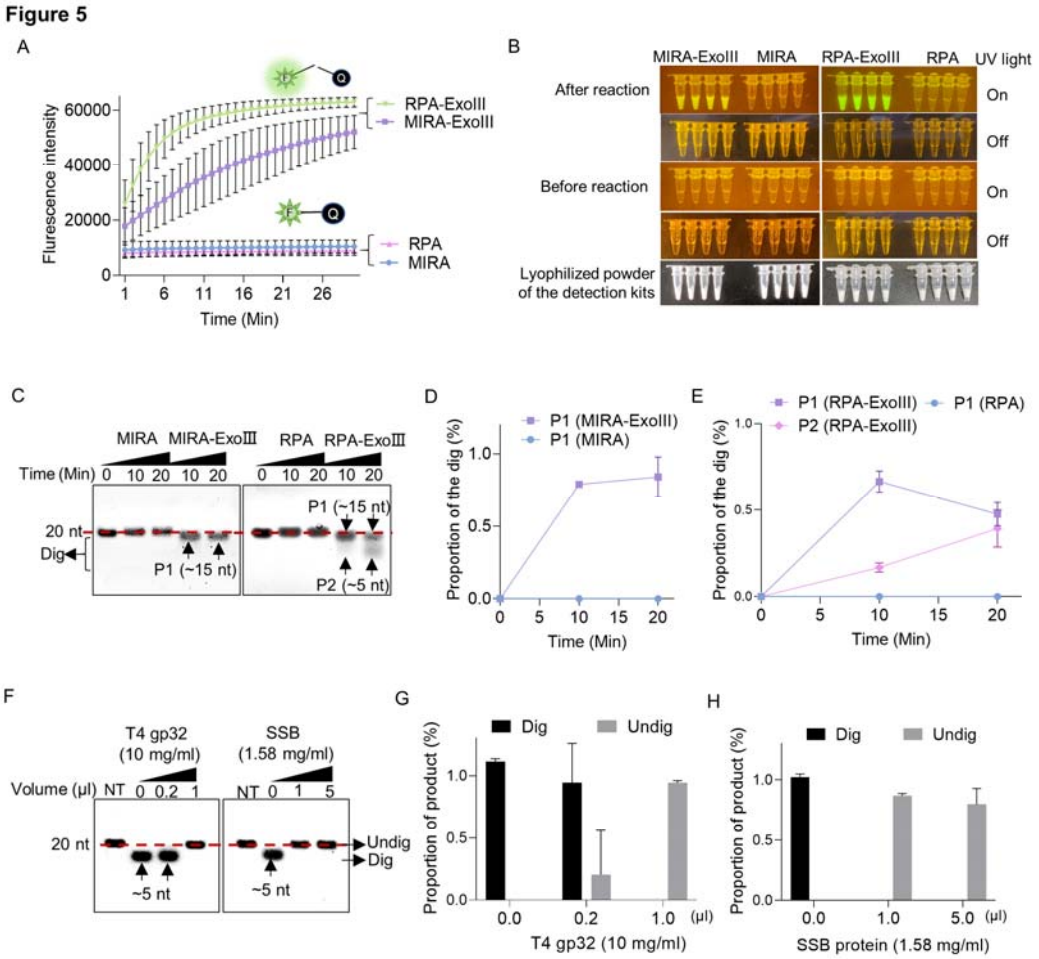

Figure 5. Exo□ in the isothermal amplification kits digested the ssDNA FQ reporter and 5′ FAM-labelled ssDNA probes, while the single-stranded DNA binding protein protected the ssDNA probe from Exo□ digestion. **(A)** The fluorescence of the FQ reporter generated in four detection kits (MIRA, MIRA-Exo□ (containing Exo□), RPA, and RPA-Exo□ (containing Exo□)) was monitored for 30 min. MIRA and RPA were the control of their corresponding counterparts, respectively. The average value of three repeats was calculated and plotted. **(B)** Before and after these four commercial kits were incubated with the FQ reporter for 30 min, the reaction tubes with fluorescence generated were visualized under LED blue light by the naked eye. MIRA-Exo□ indicates the Exo□-containing MIRA kit; MIRA indicates the MIRA kit without Exo□. **(C)** The 5′ FAM-labelled ssDNA probe (Probe 1) was incubated with the four detection kits for 20 min, and the reaction products were analyzed by gel electrophoresis. Undig, undigested; dig, digested. **(D, E)** The analysis on the gray intensities of the band was performed by ImageJ. The digested proportion was calculated by: (Intensity of the digested band)/(Intensity of the undigested band at 0 min). **(F)** Different

amounts of single-stranded DNA binding protein (T4 gp32 or SSB (*E. coli*)) were incubated with the ssDNA oligo (Probe 1) for 10 min before being treated with Exo□ for 10 min. The reaction products of Exo□ digestion were separated by gel electrophoresis. The ssDNA oligo treated with deactivated Exo□ served as control. **(G, H)** The gray intensity of bands was measured by ImageJ, and the digested or undigested proportions were calculated by: (Intensity of the digested or undigested band)/(Intensity of the band produced in the treatment of deactivated Exo□).

Figure 6

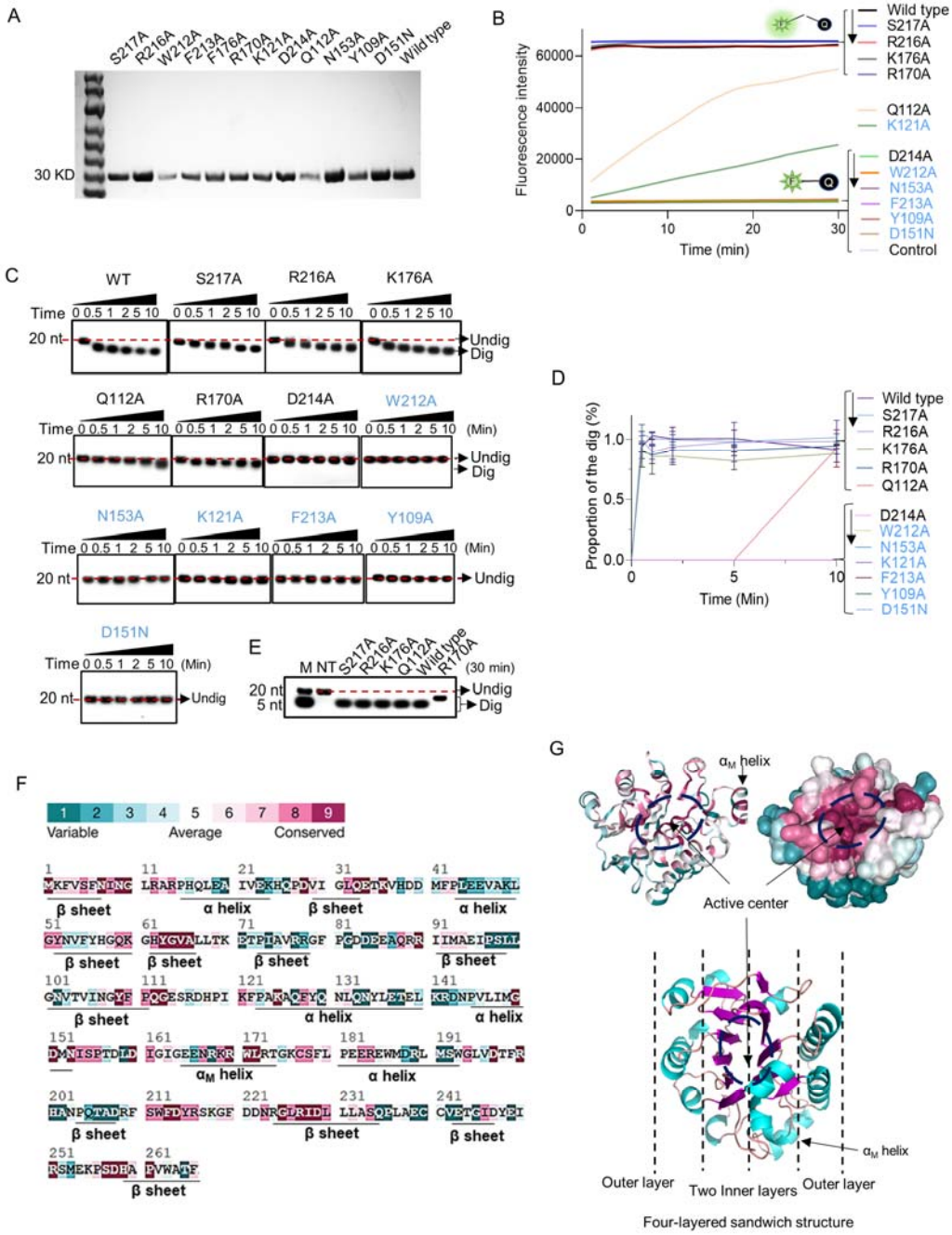

Figure 6. Point mutation of Exo□ identified the critical amino acid residues that determine the ssDNase activity. **(A)** All purified mutants and wildtype proteins used in the study were loaded into the 8% PAGE electrophoresis and stained with Coomassie Brilliant Blue. **(B)** The FQ reporter (5 μM) was incubated with Exo□ mutants (2.5 μM) (S217A, R216A, D214A, F213A, W212A, K176A, D151N, R170A, N153A, K121A, Q112A, Y109A) and wild type (WT) and the generated fluorescence was monitored for 30 min. FQ reporter treated with deactivated wildtype Exo□ was regarded as a control. The mutations in blue indicated they are previously-reportered key residues for dsDNA-targeted activities of Exo□. **(C)** The ssDNA oligo of Probe 3 (20 nt) was incubated with the Exo□ mutants, and the reaction products were analyzed by gel electrophoresis. **(D)** The gray intensity of the bands was determined by ImageJ. The average intensity value of three repeats was used to calculate the proportion of the digested band with: (Intensity of the digested band)/(Intensity of the undigested band at 0 min). **(E)** The digested products of S217A, R216A, K176A, R170A, Q112A, and wild type, after 30 min of incubation with ssDNA substrate, were compared with each other by gel electrophoresis. **(F)** The residue conservation of Exo□ (PDB ID:1AKO) was investigated using the ConSurf database (https://consurfdb.tau.ac.il/index.php). The conservation degree of Exo□ residues is calculated among 300 homologs, which the color scale indicates. **(G)** The carton and surface style of the Exo□ structure (PDB ID:1AKO) with conservation-indicated color is displayed (upper part). The four-layered sandwich structure of ExoIII is displayed by Pymol (lower part): the pink indicates β-sheet; the blue represents α-helices; the red indicates the random coils or turns.

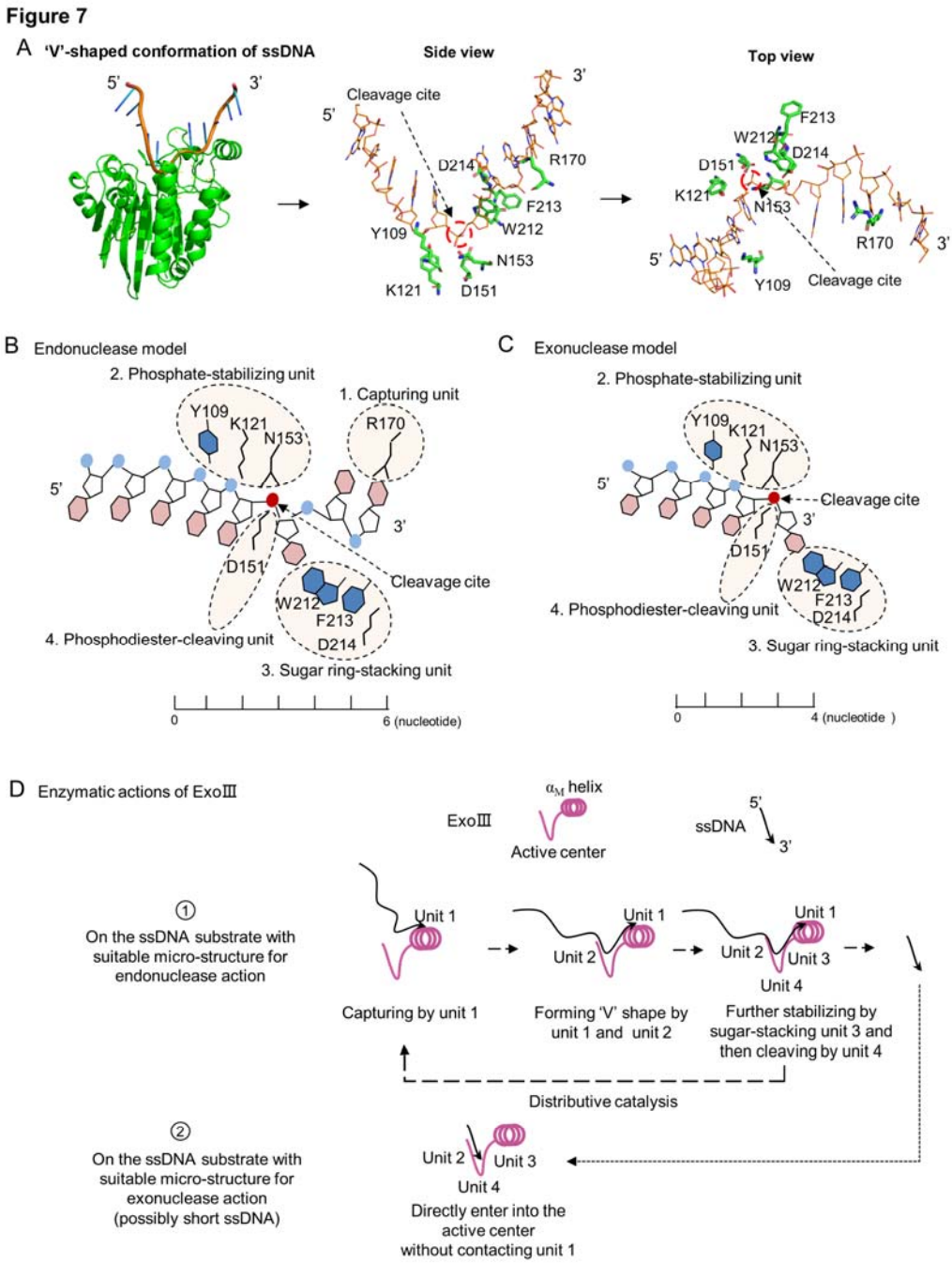

Figure 7. A theoretical model for the enzymatic actions of Exo□ on ssDNA is proposed. **(A)** The Exo□-ssDNA structure was obtained by structure alignment between Exo□ (PDB:1AKO) and APE1-dsDNA (PDB: 5WN5) by Pymol. The key residues and the cleavage site of Exo□ are labelled in situ and presented by side and top view. **(B)** According to the Exo□-ssDNA structure and the previously reported functions of the key residues (4), four functional units of Exo□ on ssDNA are primarily defined:

capturing unit (R170, at 3′ side of the cleavage site and three nucleotides away from it), phosphate-stabilizing unit (Y109, K121, and N153, at 5′ side of cleavage site and three nucleotides away from it) and sugar ring-stacking unit (W212, F213, and D214) and phosphodiester-cleaving unit (D151). In the model of endonuclease, Unit 1(R170), located at the surface of Exo□, is most likely the first contact with the substrate, and binding at the 3′ side of the cleavage site naturally drives the endonucleolytic cleavage on ssDNA. Interactions of unit 1 and unit 2 with substrates may help convert the ~6 nucleotides at 3′ end of ssDNA to form a 'V' shape intermediate for docking into the active center and being processed by unit 3 and unit 4. **(C)** In the exonuclease model, some types of ssDNA (possibly short ssDNA or others with suitable micro-structure) directly enter into the active center without contacting unit 1, and sequentially processed by unit 2, 3 and 4. **(D)** The ssDNA substrate tends to be captured by the unit 1, then stabilized by the unit 2 and 3, and finally cleaved by unit 4 of Exo□, producing short fragments of ssDNA (endonuclease activity), which may reflect the distributive catalysis of Exo□ on ssDNA. The short ssDNA (~3 nt) or others with suitable microstructure would directly enter into the active center and be processed by units 2, 3, and 4 into mononucleotides (exonuclease activity). Most ssDNA substrates might be digested by both endonuclease and exonuclease activity of Exo□.

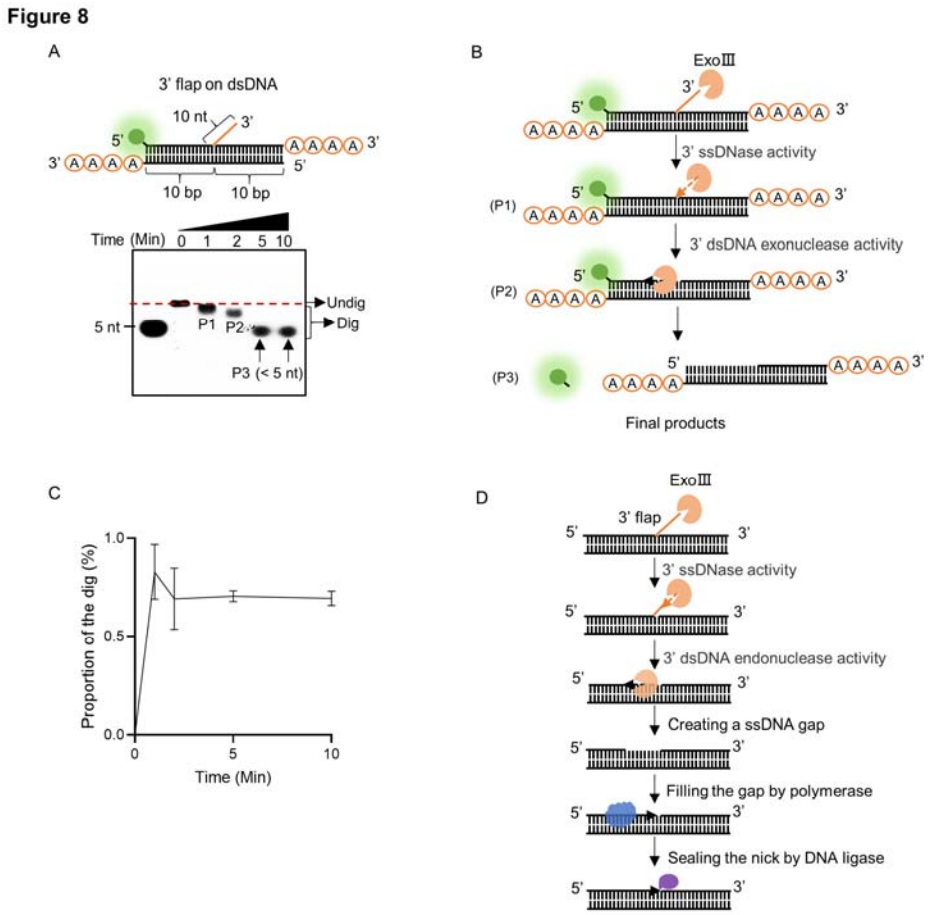

Figure 8. Exo□ efficiently digested the 3′ flap ssDNA on dsDNA. **(A)** The constitution of the dsDNA structure with 3′ flap is displayed. The time course analysis of Exo□ (2.5 μM) digestion on the structure (5 μM) was performed, and the products were analyzed by gel electrophoresis. **(B)** According to the activities of Exo□ on ssDNA and dsDNA, the process of enzymatic reaction on the dsDNA structure was outlined. **(C)** The digested proportions of ssDNA substrates were calculated by: (gray intensity of the digested band)/(gray intensity of the undigested band at 0 min) and plotted based on an average value of three repeats. **(D)** Based on our result and the gap-creation ability of Exo□ [8], a novel biological role of Exo□ in DNA repair was proposed: when the 3′ ssDNA flap occurs on dsDNA during biological processes such as BER or DNA replication, Exo□ recognizes and removes the ssDNA flap by its ssDNase activity; then it continues to digest and create a ssDNA gap on the dsDNA by exonuclease activity; the resulted intermediate recruits the DNA polymerase to re-synthesize the complementary strand; finally, the nick left is sealed by DNA ligase.